Radiation Effects & Defects in Solids
Vol. 161, No. 12, December 2006, 701–707

Taylor & Francis
Taylor & Francis Group

Angular distribution of atoms sputtered from germanium by 1–20 keV Ar ions

V. S. CHERNYSH*†, A. S. PATRAKEEV‡ and V. I. SHULGA‡

†Faculty of Physics, Moscow State University, 119992 Moscow, Russia
‡Institute of Nuclear Physics, Moscow State University, 119992 Moscow, Russia

(Received 5 May 2006; revised 18 May 2006; in final form 30 July 2006)

The angular distribution of atoms sputtered from germanium under 1–20 keV Ar^+ ion bombardment (normal incidence) has been studied experimentally and using computer simulations. A collector technique combined with Rutherford backscattering to analyze the distribution of collected material was used. In addition, the surface topography was under control. It was found that the experimental angular distribution of sputtered atoms ($E_0 = 3$–10 keV) could be approximated by the function $\cos^n \theta$ with $n \approx 1.65$. Such a high value of n is connected with the surface scattering of ejected atoms and a noticeable contribution of backscattered ions to the formation of the sputter flux (the mass effect). The target surface was found to be practically flat even at ion fluencies $\sim 10^{18}$ ions/cm^2. The results obtained are compared with data from the literature, including our recent data on Si sputtering.

Keywords: Sputtering; Angular distribution; Germanium; Experiment; Computer simulation; Surface topography

1. Introduction

The study of the angular distribution of atoms sputtered from semiconductors such as Si and Ge is of great interest to both the theory of sputtering and numerous applications. Early work on the subject revealed a wide scatter of the experimental data. For Si, for example, it was even difficult to say whether the angular spectrum of sputtered atoms is undercosine ($\cos^n \theta$, $n < 1$) or overcosine ($n > 1$). The main reason for this is probably the fact that the method of electron Auger spectroscopy, which is very sensitive to surface contaminations, was applied usually to analyze the distribution of sputtered material on a collector. In addition, in early work on Si and Ge sputtering, no control of the surface topography of the target was carried out. That is why we decided to study the problem once again both experimentally and using computer simulations. In experiments, the Rutherford backscattering (RBS) technique was used to analyze the collected material. The surface topography of the samples was studied with scanning electron microscopy (SEM) and atomic force microscopy (AFM). The simulations were carried out for amorphous target with the use of different models of the sputtering process.

*Corresponding author. Tel.: +7-495-939-2989; Fax: +7-495-939-1787; Email: chernysh@phys.msu.ru

Radiation Effects & Defects in Solids
ISSN 1042-0150 print/ISSN 1029-4953 online © 2006 Taylor & Francis
http://www.tandf.co.uk/journals
DOI: 10.1080/10420150600966059

Both primary and secondary knock-on atoms were registered. For Si targets sputtered by normally incident 1–10 keV Ar^+ ions, the results obtained were published recently in ref. [1]. The angular spectra of sputtered Si atoms were found to be overcosine with $n \sim 1.3$.

In this article, we present the experimental and computational data on sputtering of Ge targets by 1–20 keV Ar^+ ion bombardment. A special emphasis is put on the comparison of the results for Ge and Si to clarify the mechanisms of sputtering of the two materials.

2. Experiment

The sputtering experiments were carried out using a UHV setup [2] consisting of a duoplasmatron ion source, electrostatic lenses and a magnetic separator for the primary beam and a sample chamber. The (1 1 1) Ge samples were bombarded along the normal to the surface by a mass-separated Ar^+ beam with energies 3–10 keV. The ion beam density was 0.1–0.15 $\mu A/cm^2$ depending on the energy of ions. The beam diameter determined by the aperture mounted on the collector holder was 1.5 mm. Fluences of bombarding ions were about 10^{18} ions/cm^2, which is sufficient for Ge amorphization at the initial stage of irradiation. In order to achieve uniform irradiation, the ion beam was scanned over the target surface in two mutually perpendicular directions. The backsputtered material was collected on a semi-cylindrical Be foil surrounding the target. The radius of the collector was 15 mm. The distribution of the sputtered material on the collector was measured using RBS analysis with 1.5 MeV He^+ ions. The exposure to create the RBS spectrum was chosen to provide an accuracy <5% for the emission angles $\theta > 70°$, where the intensity of sputtering was low.

The surface topography of the samples was studied with the SEM LEO1455VP and the AFM Solver P47-PRO.

3. Computer simulation

The simulations were performed using the computer code OKSANA [3]. The code is based on the binary collision approximation and takes into account weak simultaneous collisions at large distances. An amorphous target is simulated by rotation of a crystalline atomic block, the procedure of rotation being repeated from collision to collision. The atomic block is chosen in the form of a tetrahedron. The standard WHB (KrC), ZBL and LJ potentials are applied as the interaction potential for colliding particles [4, 5]. The inelastic energy losses were calculated using the Firsov formula. Allowance was made for the uncorrelated thermal vibration in terms of the Debye model ($T = 300$ K). The Debye temperature for Ge is 640 K. The surface barrier was planar and the heat of sublimation (3.88 eV) was taken as the surface binding energy. A flat surface at $x = 0$ was assumed. A typical run consisted of 200,000–500,000 sputtered atoms. All other parameters were identical to the standard model [6, 7].

For better understanding of the difference between the results for Ge and Si targets, some additional simulations of sputtering were carried out for an artificial pseudo-Si target (see subsequently).

Both measured and simulated angular distributions of sputtered atoms, $Y(\theta)$ were fitted by a cosine function to the power n, namely

$$Y(\theta) \sim \cos^n \theta, \tag{1}$$

and the corresponding best-fit values of n were found.

4. Results and discussion

The normalized angular distribution of sputtered Ge atoms measured for 3 keV Ar^+ ion bombardment is shown in figure 1. As expected, the distribution is rather smooth and has no particular features typical for single crystals or textured targets. The distribution is overcosine and can be approximated well by function (1) with $n = 1.6$. For 6, 8 and 10 keV Ar^+ ions, the angular spectra are similar to those shown in figure 1; the best-fit values of the exponent n for the three energies are close to each other and lay in the narrow range of 1.6–1.7. The average value of n for all four energies is 1.66 ± 0.03.

The energy dependence of the measured values of n is shown in figure 2 together with the results of computer simulations performed using different potentials. It is seen that the simulated values of n are quite sensitive to the variation of the interatomic potential. The best agreement of the simulation results with the experimental data was obtained for the ZBL potential, whereas two other potentials lead to lower values of n. This fact can be explained by a weakness of the WHB and LJ potentials for Ge at large distances [8, figure 6], which determine the scattering of particles during their ejection from the surface. The decrease of n at low ion energies (figure 2) can be explained by a high contribution of the primary knock-on atoms, which are characterized by a much wider angular distribution.

Figure 3 compares our experimental data for Ge with the results of earlier investigations [9, 10]. Our recent data for Si [1] are also included. It is seen that all experimental values of n are in excess of the theoretical value of $n = 1$, which follows from the sputtering theories based on the model of isotropic cascade (e.g. Thompson's [11] and Sigmund's [12] theories).

Later Sigmund [13] took into account that a net noncompensated deflection of ejected atoms to the surface normal in the last collisions may transform a purely cosine angular spectrum into $\cos^n \theta$ shape with

$$n = 1 + \left(\frac{8}{3}\right) N C_0^{3/2}, \tag{2}$$

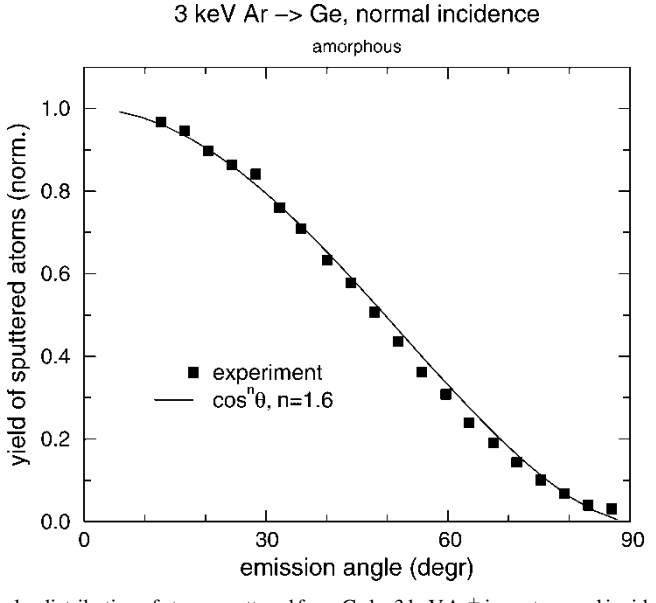

Figure 1. The angular distribution of atoms sputtered from Ge by 3 keV Ar^+ ions at normal incidence. Dots represent the experimental data; solid line is their approximation by function (1) at $n = 1.6$.

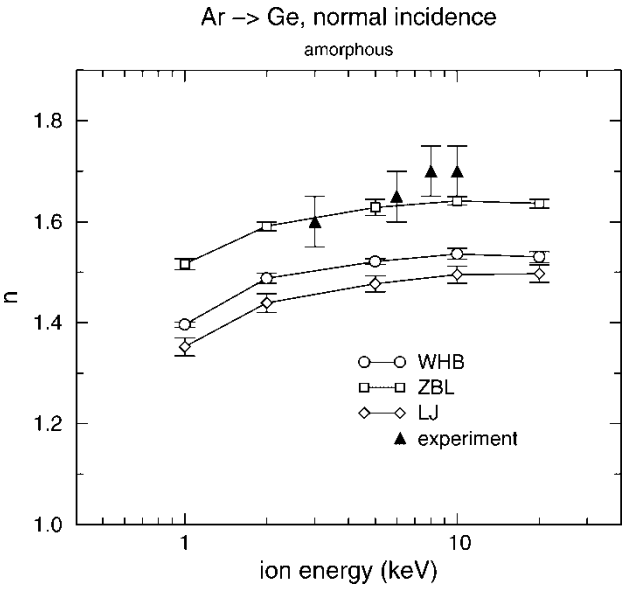

Figure 2. The energy dependences of the exponent n for an amorphous Ge target bombarded with Ar ions (normal incidence). Solid lines are the results of computer simulations performed using different interatomic potentials; dots are the experimental data.

where N is the target atomic density and C_0 the constant defined in [12]. For Si and Ge targets this estimate yields $n = 1.32$ and 1.29, respectively (the dashed and dash–dotted lines in figure 3). It is seen from figure 3 that equation (2) agrees well with the experiment in the case of Si but underestimates strongly the values of n in the case of Ge. This means that the

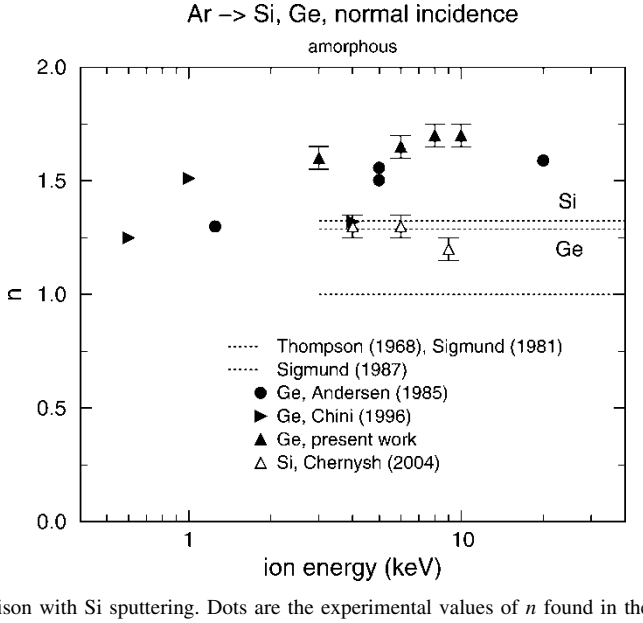

Figure 3. Comparison with Si sputtering. Dots are the experimental values of n found in the present and other works [1, 9, 10]. Dashed lines are the analytical predictions [11–13].

effect of noncompensated surface scattering alone is not enough to explain the high values of n found experimentally for Ge.

This brings up the question: what are the factors that should be taken into account to explain the experimental finding for Ge? To answer this question, a series of simulations was carried out for the so-called pseudo-Si. By a pseudo-Si is meant an usual (normal) Si target for which one of the characteristics – atomic density N, surface binding energy U, target atomic mass M_2 or target atomic charge Z_2 – is replaced by the corresponding value for Ge. For example, the change of Z_2 from 14 (Si) to 32 (Ge) leads to the variation of the two interatomic potentials (for ion–atom and atom–atom interactions) but without any changes in the values of N, U and M_2, taken as those for Si. In a similar manner, the play with M_2 may show us the mass effect in itself and so on.

The simulation results for four pseudo-Si targets and for normal Si and Ge targets are shown in figure 4 (the WHB potential). It is seen that the N- and U-effects practically compensate each other, while the M_2- and Z_2-effects are more important and, taken together, they can explain the higher n-values for Ge. The point is that Ar ions can be scattered back to the surface in a single collision from heavier Ge atoms but not from Si atoms. Moving towards the surface, such backscattered ions may create recoils oriented near the surface normal giving rise the increase of n (M_2-effect). In addition, the atom–atom scattering is much more pronounced for Ge than for Si (Z_2-effect), which amplifies the influence of surface noncompensated scattering.

Figure 5 shows the simulated values of n for different ions, from Ne to Xe. We can note a crossover of the dependencies at $E_0 \sim 3$ keV. It is seen that the energy dependence of n is less pronounced for Ne compared with all other ions, especially Xe. This result can be explained by the fact that at all energies (the light) Ne ions create more isotropic cascades.

Surface topography may change the shape of the angular distribution of sputtered atoms. It is well known that cones and pyramids can block the ejection of atoms at large emission angles, which causes the narrowing of the angular spectrum. To take into account such an effect, the surface topography of irradiated samples was studied using SEM and AFM. For Ge samples as

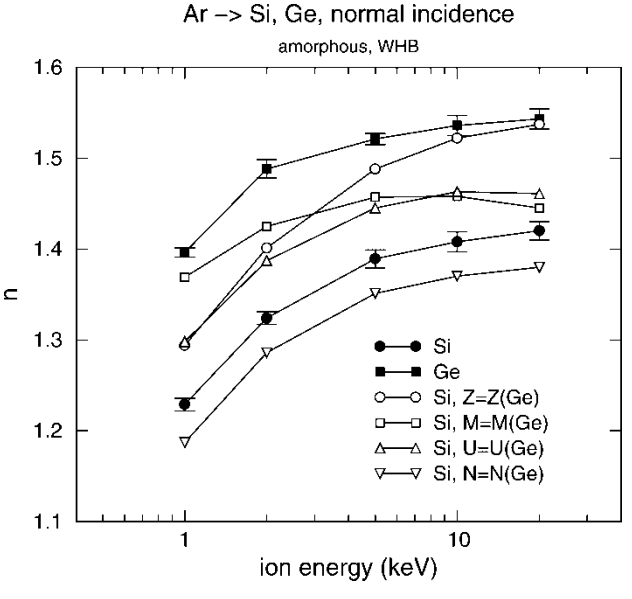

Figure 4. The energy dependences of the exponent n calculated for Si and Ge targets (the WHB potential). Also included are the results of simulations for four pseudo-Si targets (see the text).

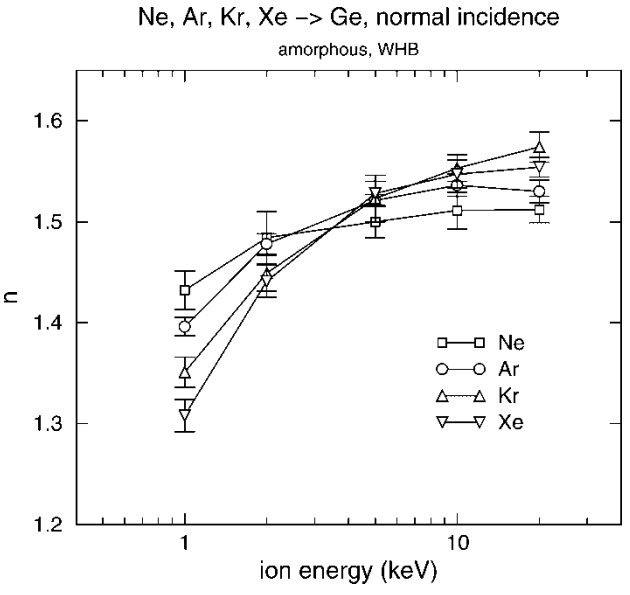

Figure 5. The energy dependences of the exponent n calculated for a Ge target bombarded with different ions.

well as for Si ones [1], SEM has not revealed the presence of any surface structures. It should be noted that for Si, we could not reveal any surface relief in the central part of bombarded spots also by the use of scanning tunneling microscopy. A rough relief [1] was observed only near the boundary of the spot. This may be connected with a low conductivity of Si samples used in our experiments (specific resistance 5 k Ω cm). However, a distinct nanorelief similar to that revealed in [14] was observed by using AFM for both Ge and Si samples. Figure 6 shows the AFM-image of Ge target after bombardment with 10 keV Ar^+ ions at fluence of about 10^{18} ion/cm^2. The figure exhibits nanohills with the average height of about 1.7 nm and the average length of 70 nm. In the case of Si, the average height and length of nanohills found for the same bombarding conditions (10 keV Ar^+) are 1.1 and 100 nm, respectively. Such a relief corresponds to a practically flat surface (the average surface curvature is about 1°–3° for Ge and Si), which cannot influence noticeably on the shape of the angular distribution of sputtered atoms.

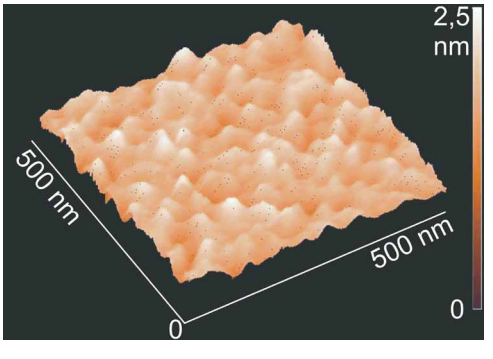

Figure 6. AFM image of a Ge surface bombarded with 10 keV Ar^+ ions.

Acknowledgements

This work was supported by Grant no. I 0751/2140 of the federal program 'Integration of Science and Higher Education on 2002–2006 years'.

References

[1] V.S. Chernysh, V.S. Kulikauskas, A.S. Patrakeev, K.M. Abdul-Cader and V.I. Shulga, Radiat. Eff. Def. Sol. **159** 149 (2004).
[2] K.F. Minnebaev, A.F. Saburov and V.S. Chernysh, Poverkhnost **11** 150 (1987).
[3] V.I. Shulga, Radiat. Eff. **70** 65 (1983).
[4] J.F. Ziegler, J.P. Biersack and U. Littmark, *The Stopping and Range of Ions in Solids*, volume 1 (Pergamon, New York, 1985).
[5] W. Eckstein, *Computer Simulation of Ion–Solid Interactions* (Springer, Berlin, 1991).
[6] V.I. Shulga and P. Sigmund, Nucl. Instr. Meth. B **119** 359 (1996).
[7] V.I. Shulga and W. Eckstein, Nucl. Instr. Meth. B **145** 492 (1998).
[8] V.I. Shulga, Nucl. Instr. Meth. B **164–165** 733 (2000).
[9] H.H. Andersen, B. Stenum, T. Sorensen and H.J. Whitlow, Nucl. Instr. Meth. B **6** 459 (1985).
[10] T.K. Chini, M. Tanemura and F. Okuyama, Nucl. Instr. Meth. B **119** 387 (1996).
[11] M.W. Thompson, Philos. Mag. **18** 377 (1968).
[12] P. Sigmund, *Sputtering by Particle Bombardment I*, edited by R. Behrisch (Springer, Berlin, 1981); Top. Appl. Phys. **47** 9 (1981).
[13] P. Sigmund, Nucl. Instr. Meth. B. **27** 1 (1987).
[14] R. Gago, L. Vazques, R. Cuerno, M. Varela, C. Ballesteros and J.M. Albella, Nanotechnology **13** 304 (2002).